Copper implantation defects in MgO observed by positron beam analysis, RBS and X-TEM

Fedorov, A.V.; Veen, A. van; Smulders, P.J.M.; Kooi, B.J.; Hosson, J.Th.M. De

Published in:
Nuclear Instruments & Methods in Physics Research Section B-Beam Interactions with Materials and Atoms

DOI:
10.1016/S0168-583X(99)00658-8

Publication date:
2000

ELSEVIER

Nuclear Instruments and Methods in Physics Research B 166–167 (2000) 225–231

NIM B
Beam Interactions with Materials & Atoms

www.elsevier.nl/locate/nimb

Copper implantation defects in MgO observed by positron beam analysis, RBS and X-TEM

M.A. van Huis [a,*], A.V. Fedorov [a], A. van Veen [a], P.J.M. Smulders [b], B.J. Kooi [b], J.Th.M. De Hosson [b]

[a] *Interfaculty Reactor Institute, Delft University of Technology, Mekelweg 15, 2629 JB Delft, The Netherlands*
[b] *Materials Science Centre, University of Groningen, Nijenborgh 4, 9747 AG Groningen, The Netherlands*

Abstract

In this work, effects of copper ion implantation in MgO were studied. (1 0 0) MgO samples were implanted with 50 keV Cu ions and thermally annealed stepwise in air for 30 minutes at 550, 750, 1000, 1250 and 1350 K. After ion implantation and after each annealing step, the samples were analysed with positron beam analysis (PBA). Use was also made of Rutherford backscattering spectrometry/channeling (RBS-C) and cross-sectional transmission electron microscopy (X-TEM). The combination of these techniques enabled to monitor the depth resolved evolution of both created defects and the copper atom depth distribution. PBA results show that copper implantation at a dose of 10^{15} ions cm^{-2} yields a single layer of vacancy type defects after annealing. However a copper implantation at a dose of 10^{16} ions cm^{-2} clearly yields two layers of defects in the material after annealing, separated by an intermediate layer. In both layers nanocavities have been identified. RBS experimental results show that the implanted copper atoms diffuse into the bulk material during annealing. X-TEM and channeling results show that after annealing, the lattice of the copper nanoprecipitates is epitaxial to the MgO host lattice. Under some circumstances, copper precipitates and small voids can co-exist. Furthermore, X-TEM measurements show that the nanocavities have rectangular shapes.

PACS: 61.72.Ww; 61.72.C; 61.82.Ms; 61.72.F
Keywords: Copper ion implantation; Nanocavities; Epitaxial precipitates; MgO

1. Introduction

Currently much research in the field of defect engineering is devoted to defects in magnesium oxide (MgO). Applications of MgO include the development of optical communications media and the use of MgO in nuclear reactor fuels. Copper, silver and gold are the most common metals used for ion implantation. The formation of metallic nanoprecipitates in MgO after implantation and subsequent annealing has been investigated for various annealing treatments using techniques such as Rutherford backscattering spectrometry/channeling (RBS-C) and optical absorption spect-

* Corresponding author. Tel.: +31-15-2781612; fax: +31-15-278-6422.
E-mail address: vanhuis@iri.tudelft.nl (M.A. van Huis).

0168-583X/00/$ - see front matter
PII: S0168-583X(99)00658-8

rometry [1]. A related topic of research is the role of cavities in the material which may act as gettering centers for implanted metal ions. Recently nanovoids in MgO have been created by helium implantation and subsequent annealing [2].

In this work, a more thorough investigation will be made to gain further insight into the nucleation, aggregation and dissociation of metallic nanoprecipitates and their possible interaction with vacancy-type defects. For this purpose, three complementary techniques were used. Positron beam analysis (PBA) is a very sensitive tool to monitor depth resolved vacancy-type defects [3]. RBS can provide information about the depth distribution of the implanted copper ions. Finally cross-sectional transmission electron microscopy (X-TEM) can provide information about the configuration of the metallic nanoprecipitates and vacancy-type defects.

2. Experimental

Two epi-polished (1 0 0) MgO samples of size $1\times10\times10$ mm^3 were implanted with copper ions at an energy of 50 keV, sample 1 with a low dose of 1.0×10^{15} ions cm^{-2} , sample 2 with a high dose of 1.0×10^{16} ions cm^{-2}. In sample 2, nanovoids were present prior to copper implantation. These nanovoids were created by 30 keV implantation of 1.0×10^{16} He ions cm^{-2} and subsequent annealing at 1350 K [2]. After copper ion implantation, the samples were annealed isothermally and stepwise in air for 30 min, at temperatures of 550, 750, 1000, 1250 and 1350 K. After each annealing step, the samples were analysed with the PBA technique using a 0–25 keV variable energy positron beam. After the 1250 and 1350 K annealing step, the 1.0×10^{16} Cu cm^{-2} implanted sample 2 was analysed using RBS-C. Finally, sample 2 was also analysed with X-TEM after the 1350 K annealing step. A reference sample was present that underwent the same treatment as sample 2, except that no pre-existent cavities were present prior to copper ion implantation. The X-TEM result of sample 2 was compared to an X-TEM analysis of sample 3. Sample 3 was implanted with 1.0×10^{16} Cu ions cm^{-2} at 50 keV energy and was subsequently annealed only at 1250 K for 30 min. Sample 3 was used in another experimental series

Table 1
Overview of sample treatment and main observations for three (1 0 0) MgO samples. Not shown is a reference sample that underwent the same treatment as sample 2, except for the fact that no pre-existent cavities were present prior to copper ion implantation

	Sample 1	Sample 2	Sample 3
Pre-existent cavities	–	1.0×10^{16} ^{3}He ions cm^{-2} and 1350 K annealing [2]	–
Implantation dose	1.0×10^{15} Cu ions cm^{-2} at an energy of 50 keV	1.0×10^{16} Cu ions cm^{-2} at an energy of 50 keV	1.0×10^{16} Cu ions cm^{-2} at an energy of 50 keV
Isothermal annealing	For 30 min at 550, 750, 1000, 1250 and 1350 K in air	For 30 min at 550, 750, 1000, 1250 and 1350 K in air	For 30 min at 1250 K in H_2/Ar gas
Positron beam analysis	• One single layer with vacancy-type defects	• Implantation created defects are dominant to pre-existent cavities • Two separated layers with large vacancy-type defects	–
RBS-C	–	• Diffusion of copper into the bulk during annealing • Copper atoms reach the cavities layers at depths over 100 nm • Copper atoms epitaxial to the MgO lattice	–
X-TEM		• Rectangular voids • No presence of copper precipitates	• Copper precipitates next to small rectangular voids

and the annealing took place in a reducing 5% H_2/95% Ar environment. However the presence of a reducing environment only affects the relative areas of the (1 0 0) and (1 1 1) facets of the copper precipitate [4]. The sample treatment is listed in Table 1.

3. Results and discussion

3.1. Positron beam analysis

The PBA results for samples 1 and 2 are shown in Fig. 1. The *S*-parameter corresponds to annihilation of positrons with conduction or valence electrons and is a strong indicator of open volume defects. On top of the figure a calculated depth distribution is shown of the copper ions after implantation and the depth distribution of implantation associated defects. These distributions were calculated with the TRIM code [5]. For comparison between the PBA data and the calculated TRIM data, the *S*-parameter has been plotted as a function of the depth in the material rather than as a function of positron energy. The depth has been calculated using the empirical relationship $\bar{z} = (\alpha/\rho)E^n$, with $\bar{z}$ the mean implantation depth in cm, E the positron energy in keV, ρ the density in g cm^{-3} and α and n are the empirical constants equal to 3.6×10^{-6} and 1.62, respectively [6].

It can be seen clearly that sample 1 (dose 1.0×10^{15} Cu cm^{-2}) results in a single layer at a depth of 0–40 nm under the surface with a quite high *S*-parameter value. These high values can only be obtained with large vacancy-type defects (size >2–5 nm), where positronium can be formed. In this layer, nanovoids and presumably copper nanoprecipitates are present. In Fig. 1, the same data are shown for sample 2 (dose 1.0×10^{16} Cu cm^{-2}). Here it can be observed that there are two peaks in the *S*-parameter graph, indicating that there are two layers of vacancy-type defects in the material, separated by a less defective layer. The formation of these two layers with vacancy-type defects does not depend on the presence of pre-existent cavities. The same PBA results were obtained for a reference sample that underwent the same treatment as sample 2 (implantation of 10^{16} copper ions cm^{-2} and annealing isothermally in air at temperatures of 550–1350 K), except for the fact that no pre-existent cavities were present prior to copper ion implantation.

In both samples 1 and 2, the defects are located deeper in the material than predicted by TRIM. This might be the result of the long-range Coulomb interactions that are typical to ionic solids such as MgO. Furthermore, it can be observed that the pre-existent cavities present in sample 2 have been 'washed out' by the copper implantation. The defects created by the copper implantation itself are thus dominant to the pre-existent cavities. The intermediate layer can be explained by assuming the presence of copper atoms, which decreases the *S*-parameter signal.

An analysis of these PBA results has been performed by employing the positron beam analysis fitting program VEPFIT [6]. For sample 1, a three-layer model is used: first a layer with 0–40 nm depth representing the implantation area, a second layer with 40–130 nm depth representing a 'tail' of defects stretching into the material and the bulk as the third layer. For sample 2, a five-layer model is used. The two peaks in the spectrum can only be ascribed to two highly damaged areas in the material, separated by a less defective layer. These are the first three layers, with boundaries at 0–15, 15–70 and 70–110 nm. Here again a tail of defects in the material is present from 110–250 nm and the fifth layer is the bulk. The *S*-parameters for each layer have been fitted and these values are plotted versus the sample treatment in Fig. 2. In the five-layer model used for sample 2, the highly damaged layers 1 and 3 behave quite similar during the annealing procedure, while the intermediate layer 2 remains stable. This implies that the vacancy-type defects in layer 1 and 3 aggregate during the annealing process, and that these big vacancy-type defects are not present in the intermediate layer.

3.2. RBS/Channeling

The high dose copper implanted sample was analysed with RBS-C to observe the depth resolved distribution of the implanted copper atoms;

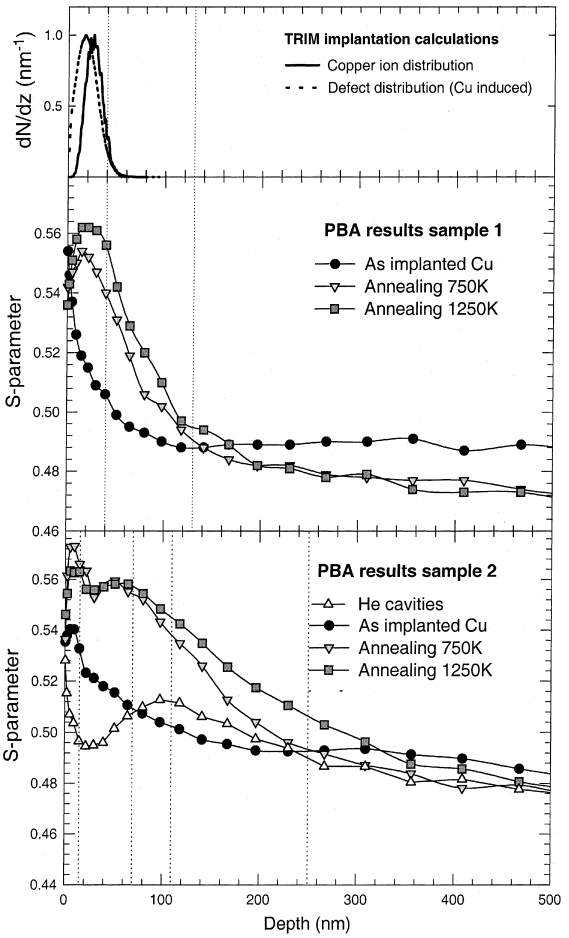

Fig. 1. TRIM calculations and positron beam analysis results. Top: TRIM predicted depth resolved distribution of copper atoms and created defects after implantation. Centre: *S*-parameter as a function of depth for sample 1 (dose 1.0×10^{15} Cu cm^{-2}) as implanted and after annealing at 750 and 1250 K. Bottom: *S*-parameter as a function of depth for sample 2 (dose 1.0×10^{16} Cu cm^{-2}) before implantation (with pre-existent cavities), as implanted with copper ions, and after annealing at 750 and 1250 K.

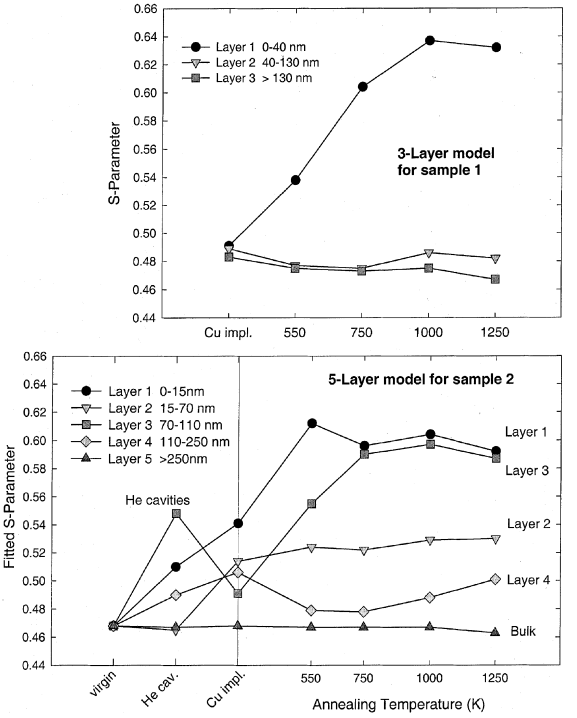

Fig. 2. VEPFIT modelled *S*-parameters in each layer versus sample treatment. The 'virgin' point is for clean unused MgO samples. Top: three-layer model for sample 1 (see text). Bottom: five-layer model for sample 2 (see text).

the result is shown in Fig. 3 and listed in Table 1. The first observation is that the copper atoms diffuse into the bulk during the annealing procedure. The total area under the signal is approximately equal for the 'as implanted' and the '1250 K annealing' case, indicating that the copper does not seggregate at the surface. Combining this with the PBA results, the copper atoms have certainly reached the 'deep' layer of nanocavities at depths over 100 nm. The second observation is that after the 1250 K annealing step, the copper atom lattice is epitaxial with respect to the MgO host lattice, as the signal is reduced to 20% when a channeling configuration is used. The X-TEM analysis that will be discussed below shows that copper nanoprecipitates are indeed epitaxial to the MgO host lattice.

3.3. Cross-sectional TEM

From the above discussion, it becomes clear that copper implantation and subsequent annealing cause a high concentration of defects that aggregate into bigger nanovoids. At the same time, the copper atoms diffuse into the bulk during the annealing process, with the copper atom lattice epitaxial to the MgO lattice. The question now

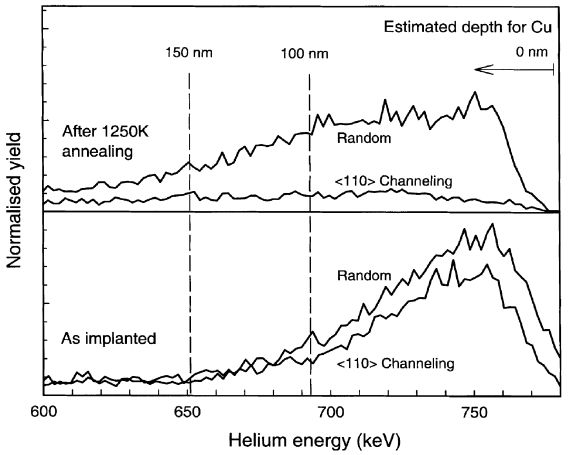

Fig. 3. RBS-C results for the of 1.0×10^{16} Cu ions cm^{-2} implanted sample 2, 'as implanted' and after the 1250 K annealing step. For both stages in the sample treatment, a random alignment (RBS) and a $\langle 1\,1\,0\rangle$ alignment (channeling) are shown.

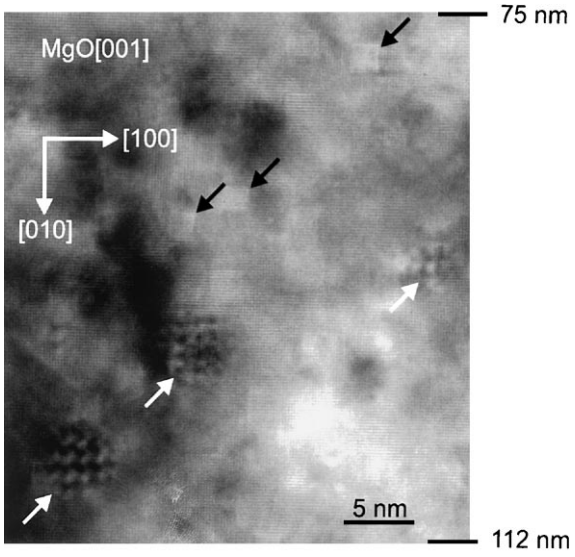

Fig. 4. X-TEM result of sample 3 after the 1250 K annealing step. Copper precipitates (white arrows) are present next to small rectangular voids (black arrows) of size 2–3 nm.

arises in what configuration the copper atoms are present during the various stages of the sample treatment. To answer this question, sample 2 was analysed using X-TEM after the 1350 K annealing step. This result was compared to the X-TEM analysis of sample 3 that was implanted with the same dose of 1.0×10^{16} copper ions cm^{-2} but was annealed only once after implantation: at 1250 K for 30 minutes in a reducing environment. The results are displayed in Figs. 4 and 5 and listed in Table 1.

Considering the X-TEM results of sample 2 (Fig. 5), it is clear that large cavities (size up to 20 nm) are present at a depth of 200–400 nm and that they are rectangularly shaped. The PBA results do not indicate large cavities at depths over 250 nm, possibly because of the low density of these defects. The rectangular shape of the cavities is probably due to the fact that the surface energy is lowest for the (1 0 0) face of MgO: the surface energy of the (1 0 0) face is calculated to be 1.2 Jm^{-2}, and the surface energy of any other (faceted) MgO surface to be at least 1.8 Jm^{-2} [7]. In sample 3 that was annealed at 1250 K in a reducing environment, nanovoids and copper nanoprecipitates co-exist and do not form common clusters. Presumably there is a bias for copper interstitial-type defects and vacancy-type defects to recombine. Furthermore, the copper precipitates seem to have a spherical shape but in fact the Cu/MgO interface consists of (1 0 0) and (1 1 1) facets [4]. In the 1350 K annealed sample 2 depicted in Fig. 4, copper nanoprecipitates can no longer be found. Possibly the copper atoms are trapped at the internal surface of the nanovoids, although this cannot be put with certainty. An order-of-magnitude calculation on the X-TEM and RBS results yields that in the high-density void areas with a void fraction of 10^{-3}, less than 10% of the internal surfaces can be covered with copper atoms. The copper atoms might also be completely dissolved in the MgO lattice, replacing certain Mg atoms. This is in some concordance with results presented by Zimmerman et al. [8] on copper precipitates in MgO. These workers observed that the absorption peak disappeared after annealing at 500 K for 1 h, assuming dissociation of the copper precipitates. In this work, the dissociation of the copper precipitates occurs only after high temperature annealing. A feasible explanation for this discrepancy is that the formation and dissociation of metal precipitates depends on the annealing time and

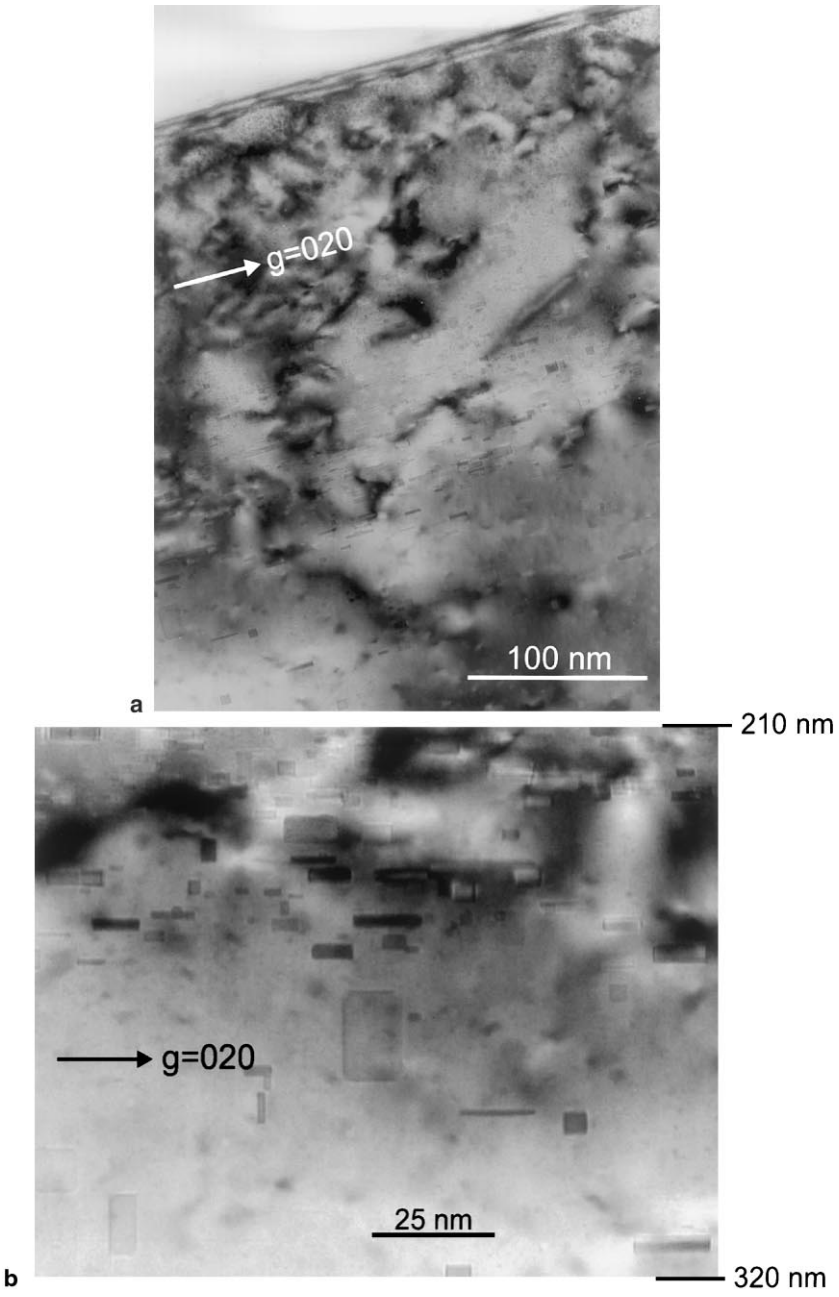

Fig. 5. X-TEM result of a high dose implanted sample after the 1350 K annealing step. (a) Overview with surface (depth up to 400 nm); (b) detail of rectangular cavities.

temperature as well as on the presence of a (non) reducing environment. The optical absorption spectroscopy technique used by Zimmerman et al. was not used in this work because the implantation doses used are too low to produce significant absorption peaks.

4. Conclusions

The major conclusions that can be drawn from the above discussion are:

- A copper implantation dose of 1.0×10^{15} ions cm^{-2} results in a single layer of nanovoids, a copper implantation dose of 1.0×10^{16} ions cm^{-2} results in two layers of nanovoids.
- The defects induced by 50 keV implantation of 1.0×10^{16} cm^{-2} copper ions dominate the presence of pre-existent nanovoids at depths over 100 nm.
- The copper atoms diffuse into the bulk during annealing, reaching the nanovoids area at depths over 100 nm.
- Copper nanoprecipitates are epitaxial to the MgO host lattice and can co-exist with nanovoids.
- Nanovoids formed in MgO are rectangularly shaped.
- After annealing at high temperature and/or for long periods of time the copper precipitates dissociate and resolve into the MgO host lattice.

References

[1] D. Ila, Z. Wu, C.C. Smith, D.B. Poker, D.K. Hensley, C. Klatt, S. Kalbitzer, Nucl. Instr. and Meth. B 127/128 (1997) 570.
[2] A. van Veen, H. Schut, A.V. Fedorov, F. Labohm, E.A.C. Neeft, R.J.M. Konings, Nucl. Instr. and Meth. B 148 (1999) 768.
[3] P.J. Schulz, K.G. Lynn, Rev. Mod. Phys. 60 (1988) 701.
[4] M. Backhaus-Ricoult, S. Laurent, Mater. Sci. Forum 294–296 (1999) 173.
[5] J.F. Ziegler, J.P. Biersack, U. Littmark, The Stopping and Range of Ions in Solids (TRIM), Pergamon Press, New York, 1985.
[6] A. van Veen, H. Schut, J. de Vries, R.A. Hakvoort, M.R. IJpma, in: P.J. Schultz, G.R. Massoumi, P.J. Simpson (Eds.), AIP 218, Positron Beams for Solids and Surfaces, 1990, p. 171.
[7] G.W. Watson, E.T. Kelsey, N.H. de Leeuw, D.J. Harris, S.C. Parker, J. Chem. Soc. Faraday Trans. 92–93 (1996) 433.
[8] R.L. Zimmerman, D. Ila, E.K. Williams, S. Sarkisov, D.B. Poker, D.K. Hensley, Nucl. Instr. and Meth. B 141 (1998) 308.